

Isolation, Characterization, and Nuclease Activity of Biologically Relevant Chromium(V) Complexes with Monosaccharides and Model Diols. Likely Intermediates in Chromium-Induced Cancers

Ruben Bartholomäus,^{†,‡} Jennifer A. Irwin,[‡] Liwei Shi,[‡] Siwaporn Meejoo Smith,^{‡,§} Aviva Levina,[‡] and Peter A. Lay^{*,‡}

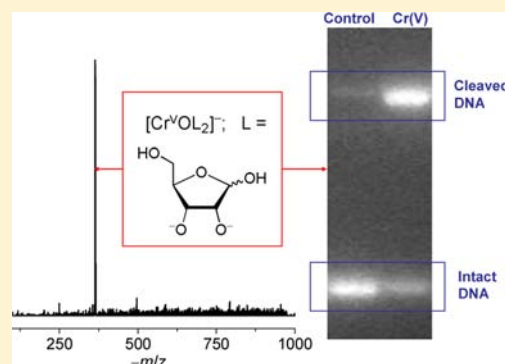
[†]Fachbereich Chemie, Philipps-Universität Marburg, Hans-Meerwein-Strasse, D-35032 Marburg, Germany

[‡]School of Chemistry, The University of Sydney, New South Wales 2006, Australia

[§]Department of Chemistry, Faculty of Science, Mahidol University, Rama VI Road, Bangkok 10400, Thailand

Supporting Information

ABSTRACT: The stabilization of Cr(V) by biological 1,2-diolato ligands, including carbohydrates, glycoproteins, and sialic acid derivatives, is likely to play a crucial role in the genotoxicity of Cr(VI) and has also been implicated in the antidiabetic effect of Cr(III). Previously, such complexes have been observed by electron paramagnetic resonance (EPR) spectroscopy in living cells or animals, treated with carcinogenic Cr(VI), as well as in numerous model systems, but attempts to isolate them have been elusive. Recently, the first crystal structure of a Cr(V) complex with *cis*-1,2-cyclohexanediol (**1**, a close structural analogue of carbohydrates) has been reported. In this work, Cr(V) complexes of the general formula $[\text{Cr}^{\text{V}}\text{OL}_2]^-$ [where $\text{LH}_2 = \mathbf{1}$, *cis*-1,2-cyclopentanediol (**2**), D-glucose (**3**), D-mannose (**4**), D-galactose (**5**), and D-ribose (**6**)] have been isolated from light-catalyzed reactions of Cr(VI) (anhydrous $\text{Na}_2\text{Cr}_2\text{O}_7$) with slight molar excesses of the corresponding ligands in *N,N*-dimethylformamide. The complexes were characterized by elemental analyses, electrospray mass spectrometry (ESMS), and EPR spectroscopy. Studies by electronic absorption spectroscopy have shown that the solids isolated from reactions of Cr(VI) with **3–6** contained mixtures of Cr(V) complexes (40–65 mol %) and Cr(III) species (probably complexes with oxidized ligands), while those from reactions with **1** and **2** were practically pure Cr(V). The first isolation of solids containing significant proportions of chromium(V) monosaccharide complexes led to the definitive assignment of their general formula $[\text{Cr}^{\text{V}}\text{OL}_2]^-$, based on ESMS, in agreement with the earlier EPR spectroscopic data. The first direct comparison of the decomposition rates of Cr(V) complexes with **1–6**, made possible by isolation of the solids, have shown that the complexes with five-membered-ring ligands (**2** and **6**) are more stable at pH ~ 7 compared with their six-membered-ring counterparts (**1** and **3–5**). This finding emphasizes the likely biological roles of chromium(V) pentose complexes, e.g., those with sugar residues of RNA, ATP, or NAD(P)H. Finally, the first direct evidence for the ability of these Cr(V) complexes to cause oxidative DNA damage in the absence of added reductants or oxidants has been obtained. These data support significant roles for chromium(V) 1,2-diolato complexes in the diverse biological activities of Cr(VI) and Cr(III).



INTRODUCTION

The potential roles of Cr(V) complexes as reactive intermediates in Cr(VI)-induced genotoxicity and carcinogenicity, first suggested by Connett and Wetterhahn in the early 1980s,¹ have since been studied in detail.^{2–6} More recently, it was suggested that the antidiabetic activities of some Cr(III) complexes⁷ also involve the formation of Cr(V) and Cr(VI) species through reactions with biological oxidants, such as H_2O_2 or ClO^- .^{8,9} Soluble Cr(VI) (in the form of $[\text{CrO}_4]^{2-}$) is efficiently taken up by cells through anion channels (because of its structural similarity to $[\text{HPO}_4]^{2-}$ and $[\text{SO}_4]^{2-}$)^{1,3} and is metabolized with the formation of Cr(III)–biomolecule complexes.^{1,10,11} The formation of Cr(V) intermediates during the biological reduction of Cr(VI) in cells and organelles,^{12–14} as well as in living plants¹⁵ and animals,^{16,17} has been observed

by electron paramagnetic resonance (EPR) spectroscopy, which is a sensitive and selective tool for the detection of Cr(V) (because of its d^1 electronic structure).^{3,5,18,19} DNA-damaging activities have been observed for some relatively stable and well-characterized Cr(V) complexes, such as $[\text{Cr}^{\text{V}}\text{O}(\text{ehba})_2]^-$ [ehba = 2-ethyl-2-hydroxybutanoate(2-)].^{20–22}

The major EPR signals ($g_{\text{iso}} \sim 1.980$), observed in Cr(VI)-treated biological systems,^{12–17} were assigned to Cr(V) complexes with highly abundant biological 1,2-diols (including carbohydrates, glycoproteins, and sialic acid derivatives), based on extensive EPR spectroscopic studies of model Cr(V) complexes.^{4,5,19,23–26} Model kinetic studies have shown that

Received: October 14, 2012

Published: March 26, 2013

significant steady-state concentrations of chromium(V) diolato complexes are expected to persist in biological systems as long as Cr(VI) is present.^{27,28} These studies were performed by the generation of Cr(V) species in solutions through reactions of Cr(VI) with large excesses of the ligands in the presence or absence of added reductants.^{23–25,29–35} This did not involve the isolation and characterization of Cr(V) complexes with biological 1,2-diols or their close structural models, cyclic *cis*-1,2-diols.^{4,5} Recently, the first complex of this kind, Na[Cr^VO(chd)₂(DMF)] (chdH₂ = *cis*-1,2-cyclohexanediol; DMF = *N,N*-dimethylformamide), was synthesized by a light-catalyzed reaction of Cr(VI) with chdH₂ in a DMF solution and was characterized by X-ray crystallography and spectroscopic techniques.³⁶ The current research expands these studies to Cr(V) complexes with a range of monosaccharides, as well as with another model ligand, *cis*-1,2-cyclopentanediol. Isolation and characterization of these complexes (of the general formula [Cr^VOL₂]⁻, where LH₂ is the ligand) led to the first direct comparison of their stability under physiologically relevant conditions, as well as to the first direct evidence of their nuclease activity, which supports their roles as likely reactive intermediates in Cr(VI)-induced DNA damage.^{2–5} Earlier studies that showed that DNA damage was caused by monosaccharide complexes were performed by *in situ* generation of the complexes by the ligand-exchange reactions of [Cr^VO(ehba)₂]⁻ with an excess of the monosaccharide ligand.^{37,38} However, these studies were ambiguous because they were complicated by the presence of excess ligand and some mixed-ligand complexes.

EXPERIMENTAL SECTION

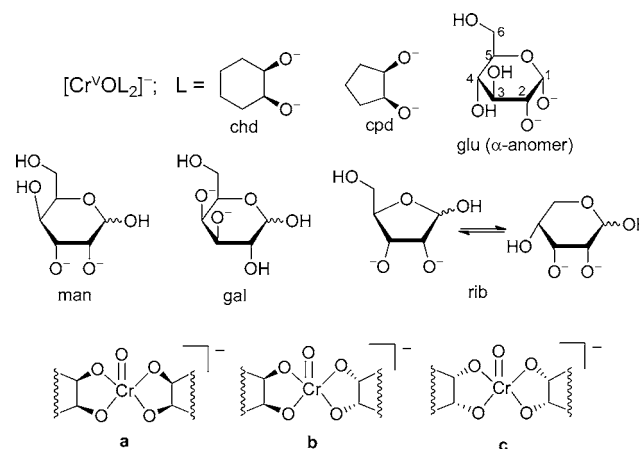
Caution! Cr(VI) compounds are human carcinogens,³⁹ and Cr(V) complexes are mutagenic and potentially carcinogenic;³ appropriate precautions should be taken to avoid skin contact and inhalation of their solutions and dusts.

Reagents and Analytical Techniques. Commercial reagents of analytical or higher purity (Aldrich, Sigma, or Merck) were used without further purification. Anhydrous Na₂Cr₂O₇ was obtained by drying the commercial dihydrate to constant mass at 378 K. The Na[Cr^VO(ehba)₂].1.5H₂O complex was used as a Cr(V) standard for EPR spectroscopic quantification and was synthesized and characterized as described previously.^{40–42} The substrates used for reactions with Cr(VI) (Chart 1) included *cis*-1,2-cyclohexanediol (chdH₂), *cis*-1,2-cyclopentanediol (cpdH₂), D-glucose (gluH₂), D-mannose (manH₂), D-galactose (galH₂), and D-ribose (ribH₂). The commercial samples were mixtures of α - and β -anomers, but gluH₂ was mainly the α -anomer. High-purity *N,N*-dimethylformamide (DMF; HPLC grade, from Aldrich) used for the syntheses and spectroscopies was kept over activated molecular sieves (4 Å). H₂O was purified by the Milli-Q technique.

The Cr content in reaction solutions and isolated solids was determined (after digestion of the samples with 69% HNO₃) by C₂H₂/air-flame atomic absorption spectroscopy (AAS), using a Varian SpecAA-800 spectrometer, calibrated with standard Cr(III) solutions (Aldrich). Elemental analyses (C, H, and N) were performed by the Australian National University Microanalytical Unit, using a Carlo Erba 1106 automatic analyzer. Electronic absorption (UV–vis) spectroscopy and kinetic studies were performed on a Hewlett-Packard HP 8452A diode-array spectrophotometer (spectral range, 200–800 nm; resolution, 2.0 nm; acquisition time, 0.20 s), equipped with an HP 89090A temperature control unit (± 0.1 K). Global analysis of the kinetic data was performed using *ProKineticist* software.⁴³ Illuminance values for the photocatalyzed reduction of Cr(VI) were measured using a EMT-201 light meter.

Continuous-wave X-band EPR spectra of Cr(V) complexes in aqueous or DMF solutions were acquired at 295 K on a Bruker EMX

Chart 1. Structures of Chromium(V) 1,2-Diolato and Monosaccharide Complexes, Showing the Main Binding Sites of the Ligands, and Possible Geometric Isomers of Cr(V) Complexes with Cyclic *cis*-1,2-Diolato Ligands (a–c)^a



^aIn addition to mixtures of geometric isomers shown in parts a–c, both *cis* and *trans* geometric isomers involving the disposition of ether linkages on the two ligands and linkage isomers can form for chromium(V) monosaccharide complexes.^{4,18,29}

spectrometer, using a Wilmad quartz flat cell; calibrations of the magnetic field and the microwave frequency were performed with an EMX 035 NMR gaussmeter and an EMX 048T microwave bridge controller, respectively. The experimental settings were as follows: center field, 3490 G; sweep width, 20–100 G; microwave frequency, ~ 9.66 GHz; modulation frequency, 100 kHz; modulation amplitude, 0.10–0.40 G; microwave power, 2.0 mW; receiver gain, 10^3 – 10^4 ; resolution, 1024 points; time constant, 20.48 ms; number of scans, 5. Aqueous solutions of Cr(V) complexes were prepared by rapid dissolution of the isolated solids in Milli-Q H₂O to [Cr] ~ 5 mM, and the spectra were acquired at 2–4 min after dissolution of the solids. An Elexsys spectrometer (Bruker, X-band), equipped with an internal NMR gaussmeter and a microwave frequency counter, was used for determination of Cr(V) in the reaction mixtures (DMF solutions) by quantitative EPR spectroscopy²⁸ and for solid-state EPR spectroscopy of Cr(V) complexes (neat isolated solids). Both types of experiments were performed at 295 K, using the settings listed above, except that the sweep width for solid-state EPR spectroscopy was 6600 G, and the modulation amplitude was 5 G. The quantitative EPR technique, validated as described previously,²⁸ involved placement of a quartz capillary containing a reaction solution (0.10 mL) inside a quartz EPR tube, together with another capillary, containing a solution of Na[Cr^VO(ehba)₂] in DMF (0.10 mL, [Cr(V)] = 10–50 mM). The $g_{\text{iso}} = 1.9780$ value for [Cr^VO(ehba)₂]⁻ in DMF solutions was in agreement with published data.⁴⁴ All EPR spectra were processed with *WinEPR*⁴⁵ and simulated with *WinSim*⁴⁶ software, respectively; second-order perturbation corrections were applied to determine the g_{iso} and A_{iso} (⁵³Cr and ¹H) values.

Electrospray mass spectrometry (ESMS) was performed using a Finnigan LCQ mass spectrometer. Typical experimental settings were as follows: sheath gas (N₂) pressure, 60 psi; spray voltage, 4.0 kV; capillary temperature, 473 K; cone voltage, 25 V; tube lens offset, 20 V; m/z range, 100–2000 (in both positive- and negative-ion modes; no significant signals were detected at $m/z > 1000$). Analyzed solutions were prepared within ~ 1 min of data acquisition at 295 K, either by dilution of the reaction mixtures with DMF or by rapid dissolution of the isolated solids in H₂O. These solutions (5 μ L, ~ 1 mM Cr) were injected into a flow of H₂O/MeOH [1:1 (v/v); flow rate 0.20 mL min⁻¹]. Acquired spectra were the averages of 10 scans (scan time, 10 ms). Simulations of the mass spectra were performed using *IsoPro* software.⁴⁷

Plasmid DNA cleavage assays and data analysis were performed as described previously.^{22,48,49} Aqueous solutions of plasmid (pUC9) DNA were a gift from Prof. N. E. Dixon, Australian National University, Canberra, Australia.

Syntheses of Chromium(V) Diolato Complexes and Isolation of Cr(V)-Containing Solids. The synthetic procedures were similar to those described previously for a crystallographically characterized complex, $\text{Na}[\text{Cr}^{\text{VO}}(\text{chd})_2(\text{DMF})]$.³⁶ For the bulk synthesis of $\text{Na}[\text{Cr}^{\text{VO}}(\text{chd})_2(\text{DMF})]$, anhydrous $\text{Na}_2\text{Cr}_2\text{O}_7$ (26.2 mg, 0.200 mmol Cr) and chdH_2 (69.7 mg, 0.600 mmol) were dissolved in DMF (2.0 mL) by vigorous stirring in a 5-mL glass vial with a plastic screw-cap and kept at 295 ± 1 K under normal laboratory fluorescent light [illuminance, $(3.0 \pm 0.5) \times 10^2$ lx]. The color of the reaction mixture changed from orange to green within several hours, and a green precipitate formed after 3 days of reaction. The precipitate was separated by vacuum filtration, washed with DMF (1.0 mL) and MeCN (3.0 mL), and dried under vacuum. Yield: 40.8 mg (52%). Anal. Calcd for $\text{C}_{15}\text{H}_{27}\text{NO}_6\text{CrNa}$: C, 45.92; H, 6.94; N, 3.57; Cr, 13.3. Found: C, 45.61; H, 6.96; N, 3.44; Cr, 13.3. The same method was used for the synthesis of $\text{Na}[\text{Cr}^{\text{VO}}(\text{cpd})_2(\text{DMF})]$, except that the precipitate was formed more slowly (5–7 days after the beginning of the reaction). Yield: 24.7 mg (34%). Anal. Calcd for $\text{C}_{13}\text{H}_{23}\text{NO}_6\text{CrNa}$: C, 42.86; H, 6.36; N, 3.84; Cr, 14.3. Found: C, 42.69; H, 6.30; N, 3.71; Cr, 14.5. Detailed spectroscopic characterizations of both complexes are given in the Results section.

Solids containing $\text{Na}[\text{Cr}^{\text{VOL}}_2]$ complexes (where LH_2 is gluH_2 , manH_2 , galH_2 , or ribH_2 ; Chart 1) were isolated from reactions of anhydrous $\text{Na}_2\text{Cr}_2\text{O}_7$ [0.10 M Cr(VI)] with the ligands (0.30 M) in DMF solutions (2.0 mL) at 295 ± 1 K and $(3.0 \pm 0.5) \times 10^2$ lx for 48 h (gluH_2 , manH_2 , and galH_2) or for 24 h (ribH_2). Small amounts of precipitates [containing mainly Cr(III)] that formed in some reaction mixtures were removed by centrifugation (5 min at 10000g). The reactions were stopped by the addition of MeCN (6.0 mL), which led to the formation of green precipitates. The precipitates were separated by centrifugation (5 min at 10000g), redissolved in DMF (1.0 mL), and reprecipitated with MeCN (3.0 mL). A similar procedure was used for isolation of a Cr(III) product from the reaction of Cr(VI) with ribH_2 , except that the reaction time was 120 h, and the solid was not redissolved in DMF. The dried precipitates were analyzed by AAS for the total Cr contents and by UV–vis spectroscopy for the relative contents of Cr(V), Cr(VI), and Cr(III) (Table 1). For the latter analyses, the solids (~1 mg) were rapidly dissolved in aqueous solutions (1.0 mL) containing equimolar amounts (0.125 M each) of ehbaH_2 and its monosodium salt ($\text{ehbaH}_2/\text{ehbaH}^-$ buffers, pH = 3.50; see the Results section for details of the analyses).

Table 1. Total Cr Content and Relative Cr(V) and Cr(III) Contents in the Solids Isolated from Reactions of Cr(VI) with Monosaccharides in DMF Solutions^a

ligand ^b	Cr_{tot}^c	$\text{Cr(V)}/\text{Cr(III)}^d$
gluH_2	9.3 (10.0)	62:38
manH_2	10.4 (10.0)	61:39
galH_2	11.0 (10.0)	65:35
ribH_2	12.3 (11.3)	41:56

^aReactions of $\text{Na}_2\text{Cr}_2\text{O}_7$ ([Cr] = 0.10 M) with the ligands (0.30 M) in DMF solutions for 48 h (gluH_2 , manH_2 , or galH_2) or 24 h (ribH_2) at 295 K and $(3.0 \pm 0.5) \times 10^2$ lx, followed by precipitation of the reaction products with MeCN (see the Experimental Section for details). ^bDesignations correspond to Chart 1. ^cTotal Cr concentrations (mass %) in the solids, determined by AAS after digestion of the samples with HNO_3 . Values in parentheses show the calculated Cr contents in $\text{Na}[\text{Cr}^{\text{VOL}}_2(\text{DMF})]$, where LH_2 is the ligand. ^dRelative contents of Cr(V) vs Cr(III) (mol % of total Cr) were determined from analysis of the UV–vis spectra obtained by dilution of the isolated solids in $\text{ehbaH}_2/\text{ehbaH}^-$ buffers (0.25 M, pH = 3.50; see the Results and Figure S1 in the SI for details). No significant amounts of Cr(VI) or Cr(IV) species were detected in the solids by this technique.

RESULTS

Generation of Chromium(V) Diolato Complexes in Nonaqueous Solutions and Isolation of Solid Products.

As described previously for chdH_2 ,³⁶ reactions of anhydrous $\text{Na}_2\text{Cr}_2\text{O}_7$ with 1,2-diols or monosaccharides (Chart 1) in DMF solutions ([Cr] = 0.040–0.10 M; [diol] = 0.12–0.40 M, ~295 K) under daylight or mild fluorescent light ($\sim 3 \times 10^2$ lx) resulted in a color change from orange ($\lambda_{\text{max}} = 374$ nm; showing a characteristic peak splitting), due to $[\text{Cr}_2\text{O}_7]^{2-}$,⁵⁰ to dark green ($\lambda_{\text{max}} \sim 600$ nm) within several hours (Figure 1a). An increase in the green color corresponded to the buildup of sharp isotropic EPR signals at $g_{\text{iso}} = 1.9795 \pm 0.0005$ and $A_{\text{iso}}(^{53}\text{Cr}) = (15.6 \pm 0.3) \times 10^{-4} \text{ cm}^{-1}$ (Figure 1b), which are characteristic of chromium(V) *cis*-1,2-diolato complexes, $[\text{Cr}^{\text{VOL}}_2]^-$ ($\text{LH}_2 = \text{diol}$).^{4,5,19} Their formation was confirmed by ESMS, which also detected the presence of Cr(VI) complexes ($[\text{Cr}^{\text{VI}}\text{O}_3(\text{LH})]^-$ and $[\text{Cr}^{\text{VI}}\text{O}_3(\text{OMe})]^-$; the latter is due to the presence of MeOH in the ESMS flushing solution), as illustrated in Figure 1c. All of these features were similar to the previously described formation of relatively stable Cr(V) complexes in reactions of Cr(VI) with thiols²⁸ or with hydroxamic acids⁵¹ in DMF solutions, except that reactions with diols were significantly catalyzed by fluorescent light, as was observed previously for reactions of Cr(VI) with peptide ligands in MeOH solutions.⁵² By contrast, extensively studied reactions of Cr(VI) with carbohydrates and their derivatives in acidic aqueous solutions led to the formation of Cr(III) products only, with Cr(V) species as unstable intermediates (observed by EPR spectroscopy).^{53–56} In particular, acid-catalyzed aqueous reactions under the published aqueous conditions^{23,44,53–56} led to the rapid decomposition of the chromium(V) diolato intermediates compared to the long lifetimes observed in DMF. Moreover, the excited-state redox potentials of Cr(VI) intermediates in nonaqueous photochemistry would be far removed from the ground-state redox potentials in acidic aqueous media or DMF, which explains the lack of reactivity of Cr(VI) with the diols in DMF in the absence of light.

The kinetics of formation and decomposition of various oxidation states of Cr during reactions of Cr(VI) with 1,2-diolato ligands in DMF solutions were studied by the additions of small aliquots of the reaction mixtures ([Cr]_{final} ~ 0.5 mM) to concentrated $\text{ehbaH}_2/\text{ehbaH}^-$ buffer solutions (0.25 M, pH = 3.50) because 2-hydroxycarboxylato complexes are more thermodynamically stable than 1,2-diolato complexes at these pH values.^{23,57} These conditions led to rapid ligand-exchange reactions of any transient Cr(V) and Cr(IV) species present in the reaction solutions to form relatively stable $\text{Cr}^{\text{V}}\text{ehba}$ and $\text{Cr}^{\text{IV}}\text{ehba}$ complexes.^{27,48,58–60} The UV–vis spectra (300–740 nm) of the four main Cr species formed under these conditions, $[\text{HCr}^{\text{VI}}\text{O}_4]^-$,⁵⁰ $[\text{Cr}^{\text{VO}}(\text{ehba})_2]^-$, $[\text{Cr}^{\text{IV}}\text{O}(\text{ehbaH}_2)]^0$, and $[\text{Cr}^{\text{III}}(\text{ehbaH})_2(\text{OH}_2)_2]^+$, are known (Figure S1a in the Supporting Information, SI).⁴² These spectra were used for multiple linear regression analyses of the UV–vis spectra observed after dilution of the reaction mixtures with an $\text{ehbaH}_2/\text{ehbaH}^-$ buffer (0.25 M, pH = 3.50; typical examples are shown in Figure S1b in the SI). The resultant spectra were unchanged for at least 15 min at 295 K, which indicates that no slower redox reactions occurred after the initial fast ligand-exchange reactions. However, it is possible that some of the initial chromium(V) monosaccharide complexes could have decomposed before the ligand-exchange reaction was complete

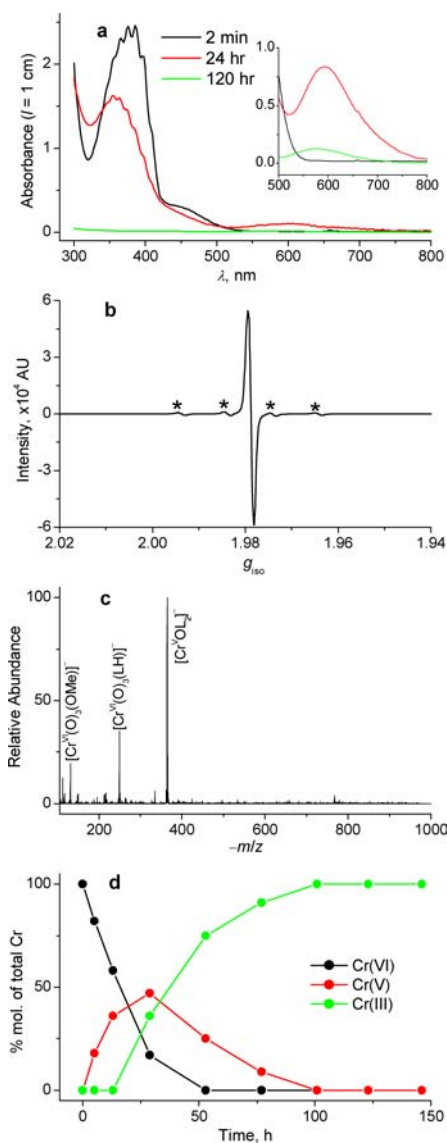


Figure 1. Typical spectroscopic and kinetic data for generation of Cr(V) complexes during reactions of Cr(VI) with *cis*-1,2-diols and monosaccharides (Chart 1) in DMF solutions: (a) time-dependent UV–vis spectra for the reaction mixtures diluted 50-fold (main part) or 5-fold (inset) with DMF [insoluble Cr(III) products formed at 120 h were removed before the dilution]; (b) solution EPR spectrum of an undiluted reaction mixture at 24 h ($g_{\text{iso}} = 1.9795$; $A_{\text{iso}}(^{53}\text{Cr}) = 15.6 \times 10^{-4} \text{ cm}^{-1}$; hyperfine splitting due to ^{53}Cr isotopes is designated with asterisks); (c) ESMS of the reaction mixture at 24 h, diluted 50-fold with DMF; (d) kinetics of formation and decomposition of Cr(V) species, determined by the dilution of aliquots of the reaction mixture with ehbaH₂/ehbaH[−] buffers (0.25 M, pH = 3.50; see the Results section and Figure S1 in SI for details). Reaction conditions: anhydrous Na₂Cr₂O₇ ([Cr] = 0.050 M); D-ribose (ribH₂, 0.15 M); 295 K; illuminance, $(3.0 \pm 0.5) \times 10^2 \text{ lx}$. See Figure S2 in the SI for the kinetic data for Cr(VI) reactions with all substrates shown in Chart 1.

because such complexes are less stable at these pH values than the model complexes. Therefore, the amount of Cr(V) determined by this method must be considered as a lower limit. No evidence for the presence of Cr(IV) species in any of the reaction mixtures was obtained. Such species would be easily detectable from the strong absorbance of Cr^{IV}ehba products at 500–600 nm (Figure S1a in the SI).^{42,48,58,60} Determination of the Cr(III) contents in the reaction mixtures

by this method was unreliable because of the relatively slow formation of Cr^{III}ehba species [because of the kinetic inertness of Cr(III)] and their low absorbances at 300–740 nm (Figure S1a in the SI). Therefore, the Cr(V) and Cr(VI) contents in the reaction mixtures were determined from the UV–vis spectra in ehbaH₂/ehbaH[−] buffers (pH = 3.50), and the Cr(III) content was then calculated from the total Cr concentrations in these solutions (determined by AAS; see the Experimental Section).

Typical kinetic curves for the various oxidation states of Cr, obtained by the above-described technique, are shown in Figure 1d [reaction of Cr(VI) with ribH₂], and those for reactions with the other ligands are shown in Figure S2 in the SI. In agreement with the earlier results,³⁶ the light-catalyzed reaction ($\sim 3 \times 10^2 \text{ lx}$, 295 K) of Na₂Cr₂O₇ (0.050 M Cr) with chdH₂ (0.15 M) in a DMF solution led to precipitation of a Cr(V) complex (Na[Cr^VO(chd)₂(DMF)]), while $\sim 40\%$ of the initial Cr(VI) remained in solution and no detectable amounts of Cr(III) were present (Figure S2a in the SI). The reaction with cpdH₂ under the same conditions (Figure S2b in the SI) led to complete conversion of Cr(VI) to Cr(V), followed by formation of a Cr(V) precipitate (Na[Cr^VO(cpd)₂(DMF)]). The purity of the products was confirmed by elemental analyses (Experimental Section) and by dissolution of the solids in ehbaH₂/ehbaH[−] buffers (250 mM, pH = 3.50, [Cr]_{final} $\sim 0.5 \text{ mM}$). The resultant UV/vis spectra corresponded to the spectrum of [Cr^VO(ehba)₂][−] (Figure S1a in the SI),⁵⁸ which indicated the absence of Cr(VI) or Cr(III) impurities. The concentrations of [Cr^VO(ehba)₂][−] in the resultant solutions were determined by UV–vis spectroscopy and agreed, within 5% experimental error, with the total Cr concentrations determined by AAS (Experimental Section). In addition, the structure of Na[Cr^VO(chd)₂(DMF)] was determined by X-ray crystallography.³⁶ Notably, no precipitates were formed during reactions of chdH₂ or cpdH₂ with K₂Cr₂O₇ under similar conditions, and the resultant Cr(V) species had to be precipitated with organic solvents.³⁶

In contrast with reactions of Cr(VI) with model 1,2-diols (chdH₂ and cpdH₂), the rates of Cr(V) formation in reactions of Na₂Cr₂O₇ with monosaccharides (gluH₂, manH₂, galH₂, and ribH₂; Chart 1) in DMF solutions were comparable with those of Cr(V) reduction to Cr(III), so that the maximal Cr(V) content in the reaction mixtures did not exceed 50 mol % of total Cr (Figures 1d and S2c–f in the SI). These results were confirmed by quantitative EPR spectroscopy of the reaction mixtures, using [Cr^VO(ehba)₂][−] in DMF as an internal standard (Figure S3 in the SI).²⁸ A good agreement (with 10% experimental error; Figure S3 in the SI) between the maximal yields of Cr(V) determined by both techniques confirmed the validity of the UV–vis spectroscopic method of Cr(V) determination (with ehbaH₂/ehbaH[−] buffer at pH = 3.50), which is much faster and easier to perform than quantitative EPR spectroscopy.²⁸ Unlike for the previous work,²⁸ constant monitoring of Cr(V) formation by EPR spectroscopy could not be used because of the slow reaction rates and need for access to fluorescent light. No improvements in Cr(V) yields were achieved by variations in the following parameters: (i) the Cr(VI) source (K₂Cr₂O₇ or (NH₄)₂Cr₂O₇); (ii) the Cr(VI)-to-ligand molar ratio (1:2 to 1:5); (iii) the amount of light (3×10^2 – $3 \times 10^3 \text{ lx}$); (iv) the reaction solvent [dimethyl sulfoxide (DMSO), acetonitrile, methanol, or acetone]. The influence of solvents on the formation of

Table 2. UV–Vis, ESMS, and EPR Spectroscopic Parameters of Chromium(V) *cis*-1,2-Diolato and Monosaccharide Complexes^a

ligand ^b	$\epsilon_{\max}(\lambda_{\max})^c$	$-m/z^d$	$A_{\text{iso}}(^{53}\text{Cr})^{e,f}$	g_{iso}^f	$A_{\text{iso}}(^1\text{H})^{f,g}$	% ^h
chdH ₂	2.6×10^2 (644)	296.2	16.0	1.9797	1.02 (2H)	59
				1.9795	0.90 (2H)	41
cpdH ₂	2.4×10^2 (600)	268.2	15.7	1.9788	0.62 (2H)	51
				1.9798	0.88 (2H), 0.73 (2H) ⁱ	49
gluH ₂	2.5×10^2 (604)	424.3	16.3	1.9790	0.97 (2H)	66
				1.9793	0.66 (2H)	26
				1.9798		8
manH ₂	3.3×10^2 (609)	424.3	16.1	1.9800	1.02 (2H)	55
				1.9796	0.85 (2H)	45
galH ₂	2.7×10^2 (613)	424.3	16.1	1.9799	0.93 (2H)	42
				1.9795	0.96 (2H)	37
				1.9793	0.88 (2H)	13
				1.9809		8
ribH ₂	3.8×10^2 (582)	364.3	15.9	1.9793	0.78 (2H)	77
				1.9800	0.82 (2H), 0.59 (2H) ⁱ	23

^aSee the Experimental Section for details of spectroscopic techniques. ^bDesignations of the ligands correspond to those in Chart 1. ^cMolar extinction coefficients ($\text{M}^{-1} \text{cm}^{-1}$) and wavelengths (in parentheses) of the absorbance maxima of Cr(V) complexes in DMF solutions [reaction mixtures were diluted 5-fold with DMF at the time when Cr(V) formation has reached its maximum; see Figures 1 and S2 in the SI]. The concentrations of Cr(V), used for calculations of the ϵ values, were determined by the addition of aliquots of reaction mixtures to ehbaH₂/ehbaH⁻ buffers (0.25 mM, pH = 3.50); see the text and Figure S1 in the SI for details. ^dValues for the main signals due to the corresponding Cr(V) species in the negative-ion mode ESMS (Figures S4 and S5 in the SI). Isolated Cr(V)-containing solids were dissolved in H₂O (to [Cr] \sim 1 mM) immediately prior to the collection of ESMS data. ^eHyperfine splitting ($\times 10^{-4} \text{cm}^{-1}$) due to the ⁵³Cr isotope (9.55% natural abundance; Figure 1b). ^fThe EPR spectroscopic parameters [g_{iso} , $A_{\text{iso}}(^{53}\text{Cr})$, and $A_{\text{iso}}(^1\text{H})$] are those of isolated Cr(V)-containing solids that were dissolved in H₂O ([Cr] \sim 5 mM) immediately prior to acquisition of the spectra (see Figure 2). The corresponding parameters of Cr(V) species formed during the reactions of Cr(VI) with the ligands in DMF solutions are listed in Table S1 in the SI. ^gSuperhyperfine splitting due to the ¹H isotope (Figure 2); the numbers of equivalent H atoms are shown in parentheses. ^hRelative abundances (mol %) of the corresponding species that give rise to the different EPR signals. ⁱSimulations of the spectra suggested the presence of two nonequivalent sets of H atoms (two atoms per set).

Cr(V) species during the reduction of Cr(VI) in nonaqueous media has been discussed in detail previously.²⁸

Solids containing Cr(V) complexes, together with significant Cr(III) [and in some cases Cr(VI)] impurities, could be isolated from the reaction mixtures in DMF by the addition of less polar organic solvents (e.g., acetone, diethyl ether, or acetonitrile). The time points when the reactions were stopped corresponded to the maximal Cr(V) contents in the reaction mixtures, as determined from the kinetic studies (Figures 1d and S2 in the SI); typically 48 h for the reactions of gluH₂, manH₂, and galH₂ or 24 h for the reactions of ribH₂. Determination of the Cr(V), Cr(VI), and Cr(III) contents was performed by dissolution of the resultant solids (to [Cr]_{final} \sim 0.5 mM) in ehbaH₂/ehbaH⁻ buffers (0.25 M, pH = 3.50), followed by analyses of the UV–vis spectra and determination of the total Cr content by AAS, as described above for the reaction mixtures (Figure S1 in the SI). The highest Cr(V) contents in the solids were achieved by the addition of three volumes of MeCN to the reaction mixtures in DMF, followed by redissolution of the resultant precipitates in DMF and reprecipitation with MeCN (Experimental Section). This procedure removed the coprecipitated Cr(VI) species and led to solids that contained at least 40–65 mol % Cr(V) (of total Cr) as well as Cr(III) species (Table 1). A similar procedure was used previously to isolate mixtures of chromium(V) and -(III) citrato complexes.⁶¹ Attempted purification of chromium(V) monosaccharide complexes by nonaqueous gel filtration chromatography⁵¹ led to their binding to the resin, followed by decomposition of Cr(V).

Characterization of Cr(V)-Containing Solids. Although high concentrations of Cr(V) species (0.050–0.10 M) could be reached during reactions of Cr(VI) with the ligands (Chart 1) in DMF solutions, isolated and dried Cr(V)-containing solids

were poorly soluble in DMF or other common organic solvents. This difference was probably due to the formation of chainlike structures in the solid state through the coordination of Na⁺ counterions to the deprotonated diolato ligands.³⁶ All of the isolated solids were well-soluble in H₂O (because the aqution of Na⁺ broke the chainlike structures), but the Cr(V) species decomposed in aqueous media within minutes under ambient conditions with the formation of Cr(VI) and Cr(III) (see below for details). The UV–vis spectral parameters of the Cr(V) species (the absorbance maxima at \sim 600 nm; Figure 1a and Table 2) were determined during generation of these species in DMF solutions, at the time points when Cr(V) concentrations reached their maximal values (Figures 1d and S2 in the SI). The Cr(VI) and Cr(III) species that were also present in solutions at these time points (except for the reaction of cpdH₂; Figure S2b in the SI) did not interfere with analysis because of their negligible absorbances at \sim 600 nm (Figure 1a). The ϵ values (Table 2) were calculated using the Cr(V) concentrations in the reaction mixtures, determined from analysis of the reaction products in ehbaH₂/ehbaH⁻ buffers (0.25 M, pH = 3.50; Figure S1b in the SI).

Negative-ion ESMS spectra of freshly prepared aqueous solutions of the isolated solids ([Cr]_{tot} \sim 1 mM; Figures 1c and S4a–f in the SI) were dominated by the signals of [Cr^VOL₂]⁻ species (where LH₂ is the ligand; see Table 2). Traces of Cr(VI) species ([HCr^{VI}O₄]⁻ and [Cr^{VI}O₃(LH)]⁻) were also detected in most of the spectra because of the rapid decomposition of Cr(V) via disproportionation in aqueous solutions. The only significant Cr-containing species detected in the positive-ion ESMS were the Na⁺ adducts of [Cr^VOL₂]⁻ (a typical example is shown in Figure S4g in the SI). Assignments of ESMS signals were confirmed by simulations of Cr isotopic patterns (Figure S5 in the SI). Despite the

significant Cr(III) content in the solids isolated from reactions of Cr(VI) with monosaccharides (Table 1), no signals of Cr(III) species were detected in ESMS probably because such species were uncharged and/or polymeric in nature. However, when the reaction of Cr(VI) with ribH₂ was allowed to proceed to complete conversion to Cr(III) (reaction time 120 h; Figure 1d), ESMS of the isolated product showed several signals assigned to Cr(III) complexes with ribonic acid (an oxidation product of ribose; Figures S4h and S5f in the SI). Polymeric chromium(III) 2-hydroxycarboxylato complexes were characterized previously as the products of Cr(VI) reduction by D-galactonic acid in aqueous media.⁵⁴

Solid-state EPR spectra of the isolated solids at either 77 K³⁶ or 295 K (Figure S6a–f in the SI) showed single sharp signals at $g \sim 1.980$, characteristic for monomeric Cr(V) complexes.^{4,5,19} A broad signal due to Cr(III) species with distorted octahedral geometry ($g \sim 2$)⁵⁴ was detectable only for the Cr^Vrib sample, which contained the highest proportion of Cr(III) (Table 1 and Figure S6f in the SI). This signal became clearly visible when the reaction was allowed to proceed to complete conversion to Cr(III) (reaction time, 120 h; Figure 1d) before isolation of the reaction product (Cr^{III}rib; Figure S6g in the SI).

Solution EPR spectra of chromium(V) 1,2-diolato complexes were collected immediately after dissolution of the isolated solids in H₂O (295 K, [Cr] \sim 5 mM, and no buffers added). The resultant spectra (Figure 2) were in agreement with the results of previous EPR spectroscopic studies, where chromium(V) 1,2-diolato complexes were generated in situ by the reactions of Cr(VI) with glutathione or other one-electron reductants in the presence of a very large (10^2 – 10^4 -fold) molar excess of the ligand.^{23–25,29–35} All of the spectra (Figure 2) showed fully or partially resolved ¹H superhyperfine splitting features, in addition to the hyperfine splitting due to ⁵³Cr (natural abundance, 9.55%; see Figure 1b).^{4,5,18,29} The g_{iso} and A_{iso} (⁵³Cr and ¹H) values, obtained from spectral simulations, are listed in Table 2, and overlays of the experimental and simulated spectra are shown in Figure 2. For all of the studied Cr(V) complexes, optimal fits were obtained by assuming the presence of two major Cr(V) species with close g_{iso} values (Table 2; details of the modeling are shown in Figure S7 in the SI). Both signals showed triplet patterns [$A_{\text{iso}}(^1\text{H}) = (0.59\text{--}1.02) \times 10^{-4} \text{ cm}^{-1}$], which arise from coupling of the d¹ electron of Cr(V) with at least two ¹H nuclei (one from each ligand), which lie within the Cr(V)–ligand plane.^{4,29,58} However, more detailed analysis with deuterated glucoses has shown that some of the apparent triplets have contributions for doublets and singlets.²⁹ In agreement with published data,^{5,31,62} the superhyperfine splitting patterns for Cr(V) complexes with five-membered-ring ligands (Cr^Vcpd and Cr^Vrib in Figure 2) pointed to the interactions of Cr(V) centers with up to four ¹H nuclei, although these interactions could not be fully resolved under our conditions (Table 2). In addition, minor Cr(V) signals were observed for the Cr^Vglu and Cr^Vgal complexes (Figure 2 and Table 2). The EPR signals gradually disappeared within 10–60 min at 295 K, in agreement with the decomposition kinetics of Cr(V) observed by UV–vis spectroscopy (see below). The EPR spectral parameters for chromium(V) 1,2-diolato and monosaccharide complexes in aqueous solutions (Figure 2 and Table 2) differed from those of the Cr(V) species formed during reactions of Cr(VI) with the ligands in DMF solutions (Figure S8 and Table S1 in the SI) by slightly higher

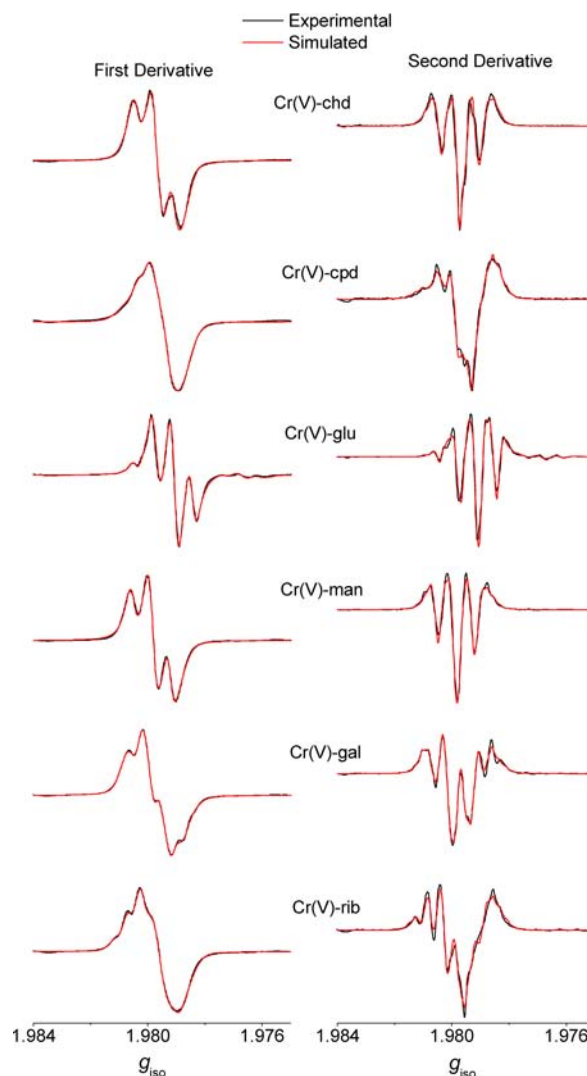


Figure 2. Experimental and simulated EPR spectra of chromium(V) *cis*-1,2-diolato and monosaccharide complexes in unbuffered aqueous solutions (pH = 6.0 \pm 0.3, 295 K). Isolated solids were dissolved in H₂O for \sim 2 min before acquisition of the spectra, [Cr]_{tot} \sim 5 mM. Designations of the ligands correspond to those in Chart 1, and simulation parameters are listed in Table 2. The EPR spectra of the corresponding Cr(V) species formed during reactions of Cr(VI) with the ligands in DMF solutions are shown in Figure S8 in the SI.

g_{iso} and A_{iso} (⁵³Cr) values (consistent with the published data of solvent dependences of EPR parameters for [Cr^VO-(ehba)₂]⁻),⁴⁴ and, in some cases, by different ratios of contributing Cr(V) species (see Tables 2 and S1 in the SI).

Decomposition and Nuclease Activity of Chromium(V) 1,2-Diolato Complexes in Aqueous Media. The decomposition rate constants of Cr(V) complexes were determined by dissolution of the isolated Cr(V)-containing solids in aqueous solutions ([Cr]_{final} \sim 0.5 mM) and following the changes in UV–vis spectra at 300–800 nm (Figures 3a and S9a in the SI). The studied conditions included phosphate buffer (33 mM, pH = 7.40, 310 K; Figure 3a), which corresponded to the conditions used in DNA cleavage studies, as well as unbuffered H₂O (pH_{final} = 6.3 \pm 0.3, 298 K; Figure S9a in the SI). In both cases, time-dependent decreases in absorbance at \sim 600 nm [due to decomposition of Cr(V)] and increases in absorbance with $\lambda_{\text{max}} = 372 \text{ nm}$ (due to the

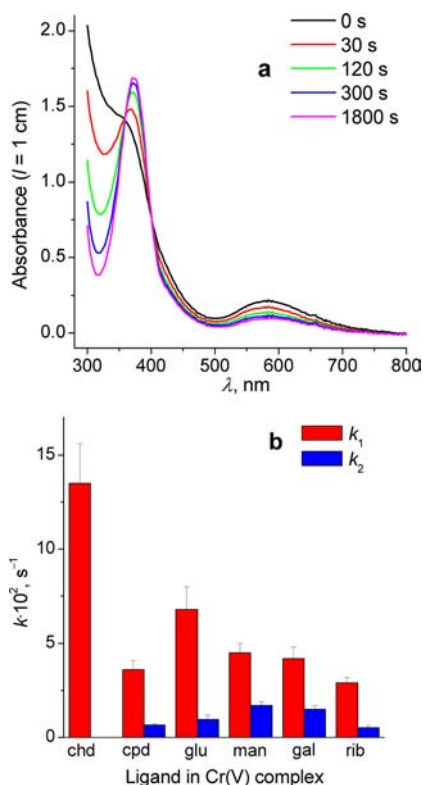


Figure 3. Kinetics of decomposition of chromium(V) *cis*-1,2-diolato and monosaccharide complexes in phosphate buffers (33 mM, pH = 7.40) at 310 K: (a) time-dependent spectra for the reaction of Cr^Vrib ($[\text{Cr}]_{\text{tot}} = 0.63 \text{ mM}$); (b) pseudo-first-order rate constants calculated by global kinetic analyses of UV-vis spectroscopic data (see Figure S10 in the SI); the average values and standard deviations for three independent kinetic experiments at $[\text{Cr}]_{\text{tot}} = 0.40\text{--}0.75 \text{ mM}$ are shown. Designations of the ligands correspond to those in Chart 1. Kinetic data for decomposition of these Cr(V) complexes in unbuffered aqueous solutions at 298 K ($\text{pH}_{\text{end}} = 6.3 \pm 0.3$) are shown in Figure S9 in the SI.

formation of $[\text{Cr}^{\text{VI}}\text{O}_4]^{2-}$ ⁶³ were observed (Figures 3a and S9a in the SI). Concentrations of Cr(VI) after complete decomposition of Cr(V) were measured by dilution of the reaction solutions with aqueous NaOH [0.10 M; $\epsilon([\text{Cr}^{\text{VI}}\text{O}_4]^{2-}) = 4.81 \times 10^3 \text{ M}^{-1} \text{ cm}^{-1}$ at pH = 13].⁶³ The total Cr concentrations were determined by AAS, and the initial Cr(V) contents in the solids (Table 1) were determined with the use of ehbaH₂/ehbaH⁻ buffers (0.25 M, pH = 3.50), as described above. These measurements showed that, under all of the studied conditions, the amounts of Cr(VI) formed during decomposition of Cr(V) were $66 \pm 5 \text{ mol } \%$ of the initial amount of Cr(V), which means that Cr(V) decomposed almost exclusively by disproportionation ($3\text{Cr}^{\text{V}} \rightarrow 2\text{Cr}^{\text{VI}} + \text{Cr}^{\text{III}}$).⁴⁸ This behavior is similar to that of the well-studied chromium(V) 2-hydroxycarboxylato complexes over the same pH range,⁴⁸ while Cr(V) complexes with other types of biologically relevant ligands (hydroxamic acids or glutathione) decomposed predominantly by ligand oxidation.^{51,64}

The kinetics of Cr(V) decomposition reactions were studied by global kinetic analysis^{27,48,65} of the UV-vis spectroscopic data obtained over the range 300–800 nm; typical results are shown in Figure S10 in the SI. Excellent fits of the time-dependent spectral changes were obtained by using two sequential pseudo-first-order reactions (Figure S10c,d in the SI), with the exception of a fast reaction of Cr^Vchd in

phosphate buffer at pH = 7.40, where only one rate constant could be discerned (Figures 3b and S9b in the SI). Calculated spectra of the reaction intermediates (Figure S10a,b in the SI) were distinguished from those of the final products by increased absorbances at ~300 nm, which is consistent with the formation of transient monoligated Cr(V/IV) species.⁴⁸ The same trends in the relative stabilities of Cr(V) complexes were observed both in phosphate buffers (pH = 7.4; Figure 3a) and in unbuffered aqueous solutions (pH = 6.3 ± 0.3 ; Figure S9a in the SI): the Cr^Vchd complex was the least stable one, followed by Cr^Vglu, Cr^Vgal \approx Cr^Vman, Cr^Vcpd, and Cr^Vrib. Notably, the two most kinetically stable complexes were those with five-membered-ring ligands (Chart 1).

Reactions of freshly prepared solutions of chromium(V) diolato complexes ($[\text{Cr}^{\text{V}}]_0 = 0.50$ or 1.0 mM , adjusted for the Cr(V) content in the isolated solids; see Table 1) with supercoiled plasmid pUC9 DNA ($20 \mu\text{g mL}^{-1}$) in phosphate buffers (33 mM, pH = 7.40, 1 h at 310 K) led to concentration-dependent levels of single-stranded breaks (SSBs), which were detected from increases in the relative concentrations of relaxed (form II) over supercoiled (form I) DNA (Figure 4a,b).^{20–22}

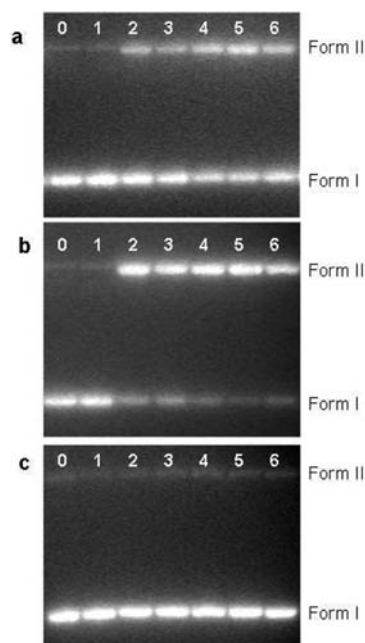


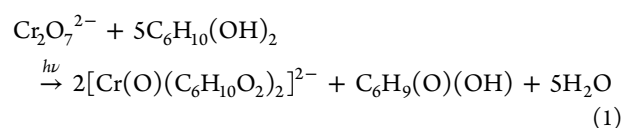
Figure 4. Typical results of plasmid DNA cleavage experiments ($20 \mu\text{g mL}^{-1}$ of pUC9 DNA, 33 mM phosphate buffer, pH = 7.40, 1 h at 310 K): (a) $[\text{Cr}^{\text{V}}]_0 = 0.50 \text{ mM}$, fresh solutions; (b) $[\text{Cr}^{\text{V}}]_0 = 1.0 \text{ mM}$, fresh solutions; (c) $[\text{Cr}^{\text{V}}]_0 = 1.0 \text{ mM}$, decomposed solutions (reacted with the buffer for 1 h at 310 K prior to the addition of DNA). The concentrations of chromium(V) carboxylato complexes were adjusted for Cr(V) content in the isolated products (Table 1). Designations of the lines are as follows: 0 is the negative control ($[\text{Cr}]_{\text{tot}} = 0$); 1 is Cr^Vchd ($[\text{Cr}]_{\text{tot}} = 0.50$ or 1.0 mM); 2 is Cr^Vcpd ($[\text{Cr}]_{\text{tot}} = 0.50$ or 1.0 mM); 3 is Cr^Vglu ($[\text{Cr}]_{\text{tot}} = 0.80$ or 1.6 mM); 4 is Cr^Vman ($[\text{Cr}]_{\text{tot}} = 0.80$ or 1.6 mM); 5 is Cr^Vgal ($[\text{Cr}]_{\text{tot}} = 0.75$ or 1.5 mM); 6 is Cr^Vrib ($[\text{Cr}]_{\text{tot}} = 1.2$ or 2.4 mM).

The same trend in the extent of DNA cleavage was observed at both Cr(V) concentrations (Figure 4a,b): Cr^Vchd < Cr^Vcpd \approx Cr^Vglu < Cr^Vman \approx Cr^Vgal \approx Cr^Vrib. No significant DNA cleavage by Cr^Vchd was observed (lines 1 in Figure 4a,b), which is consistent with the low stability of this complex in aqueous solutions (Figures 3 and S9 in the SI). As shown in Figure 4c,

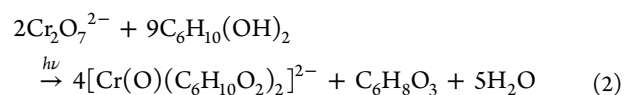
no DNA cleavage was observed when decomposed solutions of Cr(V) complexes were used (reacted with the buffer for 1 h at 310 K prior to the addition to DNA; see the decomposition kinetics in Figure 3). These results show that neither Cr(VI) nor Cr(III) [formed during the decomposition of Cr(V) or present in the solid samples; Table 1] caused the nuclease activity. Like the previous results with $[\text{Cr}^{\text{V}}\text{O}(\text{ehba})_2]^{-20-22}$ and unlike for reactions of Cr(VI) in the presence of biological reductants,⁶⁶⁻⁶⁸ DNA cleavage by chromium(V) 1,2-diolato complexes was not inhibited by catalase (up to 50 $\mu\text{g mL}^{-1}$), which shows that cleavage is likely to be caused by direct reactions of Cr(V) with DNA rather than by the formation of reactive oxygen species.^{2,22,69} These species are most likely to be peroxido complexes with ascorbate and other biologically relevant ligands.⁷⁰

DISCUSSION

Cr(V) complexes with biological and model 1,2-diolato ligands [generated in situ by reactions of Cr(VI) with large excesses of ligands in the presence or absence of added reductants] were extensively studied previously by EPR spectroscopy.^{4,5,19,26} Nevertheless, the first isolation of solids containing these complexes as major components [in mixtures with Cr(III); Table 1] reported herein led to a significant expansion of our knowledge on these biologically significant important compounds. The isolated chromium(V) monosaccharide complexes included those with predominantly *cis*-1,2-diolato moieties in the 1,2, 2,3, or 3,4 positions of the sugar ring [although minor chromium(V) *trans*-1,2-diolato species are also present],^{4,18,29} as well as those with the ligands in predominantly hexose or pentose forms (see Chart 1). It was also possible to compare the properties of such complexes with those of Cr(V) complexes with model *cis*-1,2-diolato(2-) ligands (chd and cpd; Chart 1), which could be isolated in a pure form (Experimental Section). The stoichiometry of these complexes ($[\text{Cr}^{\text{V}}\text{OL}_2]^-$, where LH_2 is the ligand), which was assigned previously on the basis of EPR spectroscopy,^{4,5,18,19,29} has been confirmed for the first time by ESMS (Figures 1c and S4 and S5 in the SI). Previously, ESMS could not be performed because of the presence of high excess concentrations of ligands and buffer ions in the reaction mixtures. In the reactions of these ligands with Cr(VI) in aprotic solvents, the ground-state redox potential of the Cr(VI/V) couple is very difficult to measure because it involves transient chromium(VI) ester intermediates and the redox reaction is irreversible. However, it is clearly insufficient for the reaction to occur at any appreciable extent. This redox reaction can be accelerated by the addition of acid to DMSO solutions,⁷¹ but this only results in Cr(III) products because the acid also destabilizes Cr(V) intermediates. In order to synthesize the desired Cr(V) complexes as kinetically stable products for simple diols or as moderately stable intermediates for the monosaccharide complexes, photochemical reactions were employed. For these reactions, it is even more difficult to ascertain the excited-state redox potentials for reduction of the chromium(VI) ester intermediates than it is for the ground-state redox couples. However, it is clear that the excited states of the Cr(VI) intermediates are much more powerful oxidants than are the ground states of the complexes and, hence, greatly accelerate the reaction without the need to add acid. The protons required for redox reactions are supplied by diol ligands themselves according to the stoichiometry of the reactions:



and/or



The nature(s) of the final organic products have not been analyzed, but the same desired Cr(V) products are formed in either reaction. While the Cr(V) redox reactions are also light-catalyzed, these are not as sensitive as the Cr(VI) reactions and, hence, by careful monitoring of the kinetics of the reaction (Figure 1), it is possible to isolate analytically pure (micro-analysis, ESMS) Cr(V) products with simple cyclic diols and maximize the percentage of chromium(V) monosaccharides in the products.

The reasons for the difficulty in being able to obtain pure solids of the monosaccharide complexes under conditions that produced pure solids of the complexes with cyclic *cis*-diolato ligands are probably severalfold: (i) the noncoordinating alcohol donors of the monosaccharides could interfere with the formation of insoluble chain structures³⁶ by coordinating to the cations that normally form bridges and/or offer steric hindrance to the formation of such bridges; (ii) the large number of linkage isomers that are possible makes it less likely for a particular isomer to precipitate; (iii) the electron-withdrawing effects of the ring oxygen and the uncoordinated alcohol groups would weaken the Cr–O bonds and make the $[\text{Cr}^{\text{V}}\text{OL}_2]^-$ intermediates more susceptible to secondary photochemistry than with simple diolato ligands. The lack of changes in the percentage of Cr(V) in the product with changes in the ligand concentration is explained by the slow rate-determining step of photoreduction of Cr(VI) to Cr(V). The ligand does not need to be in a large excess to stabilize Cr(V) because it was shown herein by EPR spectroscopy that, even in the absence of excess ligand (and the absence of light), these Cr(V) species are stable for over 1 week in DMF. Thus, photoreduction of the Cr(V) intermediates to Cr(III) is independent of the ligand concentration (over the range studied) and results in the same ligand-independent Cr(V)/Cr(III) ratio profile.

The presence of sugar anomers in the reactants contributed to the complexity of the EPR spectra of their Cr(V) complexes. However, the rates of mutarotation at 295 K in DMF are extremely low and occur over many weeks for sugars such as gluH2.⁷² It is consistent with a lack of change in the shapes of the Cr(V) EPR peaks with time in DMF. Previously, it was shown that these EPR signals are sensitive to mutarotations, which change the ratio of anomers in water,²⁹ and explains changes in the coupling patterns in water compared with DMF.

Complexes of Cr(III) with 2-hydroxycarboxylic acids (carbohydrate oxidation products) were the likely coprecipitates isolated with chromium(V) carbohydrato complexes (based on ESMS data; Figures S4h and S5f in the SI). Complexes of Cr(III) with biological 2-hydroxycarboxylates, such as citrate, are well-known.⁶¹ The absence of significant amounts of Cr(VI) in the products was due to the choice of reaction times from the kinetic studies (Figures 1d and S2 in the SI) and higher solubility of Cr(VI) in organic solvents (DMF and MeCN; see the Experimental Section) compared

with Cr(V) or Cr(III). The absence of Cr(IV) species in the products was consistent with their generally lower stability compared with related Cr(V) complexes, which is particularly pronounced in the case of 1,2-diolato(2-) ligands.⁶⁰ The presence of very small amounts of uncoordinated organic matter in the form of unreacted ligands and/or of their oxidation products in the isolated solids could not be excluded. However, the total amount of Cr in the isolated solids, which were close to those calculated for pure Cr(V) complexes (Table 1), precludes any significant contamination.

The $[\text{Cr}^{\text{V}}\text{OL}_2]^-$ complexes can exist in the form of several geometric and linkage isomers (e.g., parts a–c in Chart 1b),^{4,5,29} where the structure a corresponds to the $\text{Na}[\text{Cr}^{\text{V}}\text{O}(\text{chd})_2(\text{DMF})]$ complex, determined by X-ray crystallography.³⁶ However, the current EPR spectroscopic studies (Table 2 and Figure 2), as well as the earlier studies,^{4,29} showed that chromium(V) *cis*-1,2-diolato and monosaccharide complexes exist as mixtures of at least two geometric (and often linkage) isomers in aqueous solutions. The EPR signals of these isomers were simulated as triplets with similar g_{iso} values and indistinguishable A_{iso} (⁵³Cr) values (Table 2). The g_{iso} values for the isomers of $\text{Cr}^{\text{V}}\text{glu}$ were slightly lower than the corresponding values for the other complexes (Table 2) because of the closer proximity of the electron-withdrawing endocyclic O atom of the ligand to Cr(V).^{4,29} In agreement with earlier data,³¹ a more complicated pattern of super-hyperfine splitting was observed for the complexes with five-membered-ring ligands (cpdH_2 and ribH_2 ; Chart 1) compared with those with six-membered-ring ligands, probably because of the greater rotational flexibility of the former complexes. The minor signals detected in the EPR spectra of $\text{Cr}^{\text{V}}\text{glu}$ and $\text{Cr}^{\text{V}}\text{gal}$ (Table 2 and Figure 2) were attributed to less thermodynamically stable Cr(V) complexes with *trans*-1,2-diolato or 1,2,4-triolato forms of the ligands.^{4,29} More complicated patterns in the EPR spectra of chromium(V) monosaccharide complexes (arising from linkage isomers) were observed previously using high-field EPR spectroscopy and deuterated ligands,²⁹ but these were not resolved under the conditions of this work. Detailed speciation will be reported elsewhere.^{29b} Small differences (within 0.0005 units) between the g_{iso} values reported here (Table 2) and previously published data^{5,29} were probably due to the differences in instrument calibration, but trends in the changes of these values between the Cr(V) complexes with various ligands remained the same.

The isolation of chromium(V) *cis*-1,2-diolato and monosaccharide complexes allowed for a direct comparison of the relative stabilities of these compounds in aqueous solutions (Figures 3 and S8 in the SI), by avoiding the simultaneous formation and decomposition of Cr(V) complexes, which was inevitable under the in situ generation conditions. The decomposition rates of these complexes in either buffered (pH = 7.40; Figure 3) or unbuffered (pH = 6.3 ± 0.3; Figure S9 in the SI) aqueous solutions correlated roughly with the absorbance maxima in their UV–vis spectra (in DMF solutions), where the higher λ_{max} values corresponded to lower donor strengths of the alcoholato donor groups and consequently to higher decomposition rates of the complexes (Table 2 and Figures 3 and S8 in the SI). However, the energy of this transition is also sensitive to the degree of distortion from the ideal square-pyramidal and trigonal-bipyramidal structures.^{41,59} The higher aqueous stability of Cr(V) complexes with five-membered-ring ligands (cpdH_2 and ribH_2 ; Chart 1), compared to those with six-membered-ring

ligands, is likely to be due to the preferred bite angles in the former complexes. Notably, the $\text{Cr}^{\text{V}}\text{chd}$ complex is the only one for which a crystal structure has been obtained to date³⁶ and is also the least stable one in aqueous media (Figures 3b and S8b in the SI). The higher stability of a Cr(V) complex with D-ribose compared with those of other monosaccharides in neutral aqueous solutions (Figures 3b and S9b in the SI) suggests that D-ribose residues of such ubiquitous biomolecules as RNA, ATP, and NAD(P)H play a larger role than previously recognized^{3,4} in the intracellular stabilization of Cr(V) species.

The stoichiometry ($3\text{Cr}^{\text{V}} \rightarrow 2\text{Cr}^{\text{VI}} + \text{Cr}^{\text{III}}$; see the Results section) and kinetics (time-dependent UV–vis spectra modeled by two sequential pseudo-first-order reactions; Figure S10 in the SI) of Cr(V) decomposition, observed in this work, were similar to those reported previously for $[\text{Cr}^{\text{V}}\text{O}(\text{ehba})_2]^-$.⁴⁸ In a manner similar to that of the latter complex, chromium(V) *cis*-1,2-diolato and monosaccharide complexes are likely to decompose through a complicated mechanism involving monoligated Cr(V/IV) intermediates,⁴⁸ but detailed studies of this mechanism were outside the scope of the current work. Reactions of $[\text{Cr}^{\text{V}}\text{O}(\text{chd})_2]^-$ and $[\text{Cr}^{\text{V}}\text{O}(\text{cpd})_2]^-$ complexes with thiols led to the formation of chromium(V) thiolato and mixed chromium(V) diolato–thiolato complexes.²⁸ Similarly, decomposition of chromium(V) 1,2-diolato complexes in biological media, in the presence of numerous other types of ligands, is likely to lead to the formation of Cr(V) ligand-exchange products.⁶¹ Among the possible targets for such reactions are the Cys residues in the active centers of protein tyrosine phosphatases and other regulatory enzymes.^{8,73} The resulting changes in cell signaling are likely to contribute to the insulin-enhancing activity of Cr(III) complexes, which is most consistently observed under the conditions that favor Cr(III) oxidation to Cr(V) and Cr(VI) species.⁷³ Other likely targets are the Cys residues of Zn finger proteins,⁷⁴ which can contribute to disruptions in DNA–protein interactions and in DNA repair that are observed in Cr(VI)-treated cells and organisms.^{75,76}

Finally, isolation of chromium(V) *cis*-1,2-diolato and monosaccharide complexes allowed for the first direct observation of their nuclease activity in neutral aqueous media (Figure 4). Such observations were not possible using in situ generated Cr(V)^{4,5,29} because of the presence of large excesses of the ligands (which inhibit DNA cleavage)²² and of the Cr(VI) + reductant systems (which may cleave DNA in their own right).³ The extents of pUC9 plasmid DNA cleavage for all of the studied complexes, except for $\text{Cr}^{\text{V}}\text{chd}$ (Figure 4), as well as their decomposition rates under the conditions of DNA cleavage (Figure 3), were similar to those observed previously for $[\text{Cr}^{\text{V}}\text{O}(\text{ehba})_2]^-$.²² The lower extent of DNA cleavage by $\text{Cr}^{\text{V}}\text{glu}$ compared with other chromium(V) monosaccharide complexes (Figure 4a,b) correlates with the highest decomposition rate of $\text{Cr}^{\text{V}}\text{glu}$ among such complexes (Figures 3 and S9 in the SI). This effect is also in agreement with the lowest g_{iso} value of the main $\text{Cr}^{\text{V}}\text{glu}$ species ($g_{\text{iso}} = 1.9790$; see Table 2), arising from Cr binding to the 1 and 2 positions of α -D-glucose (Chart 1),²⁹ as a result of the strongest inductive substituent effect of the ligands.⁷⁷ The extents of DNA cleavage by Cr(V) complexes with monosaccharides (except for D-glucose) appeared to be higher than that for a model $\text{Cr}^{\text{V}}\text{cpd}$ complex (Figure 4a,b), possibly because of hydrogen-bonding interactions between OH groups of monosaccharide ligands and phosphate groups of the DNA chain. However, further studies are required to establish

whether these differences were statistically significant. As is clearly demonstrated in the present work, Cr(V) complexes, rather than their decomposition products [Cr(VI) and Cr(III) species], were responsible for causing SSBs in plasmid DNA (Figure 4b,c). Oxidative DNA cleavage is unlikely to be the main mode of DNA damage by chromium(V) 1,2-diolato complexes formed in living cells because of the abundance of potential inhibitors in a cellular medium.²² However, the ability of chromium(V) monosaccharide complexes to cause SSBs in vitro is a good indicator of the ability of such complexes to cause other forms of DNA damage in vivo, including abasic sites and Cr^{III}DNA adducts.^{10,27,78}

In summary, the results of DNA cleavage experiments support the hypothesis^{4,27} that Cr(V) complexes of biological 1,2-diols, formed during reactions of Cr(VI) with biological reductants in the presence of excess diols, are likely to be involved (both directly and indirectly) in Cr(VI)-induced DNA damage. The involvement of Cr(V) intermediates in such damage has been disputed based on the results of in vitro studies, which suggested that reactions of Cr(VI) with major cellular reductants (ascorbate, cysteine, or glutathione) led to the formation of relatively kinetically labile Cr(III) intermediates that bind to DNA, followed by the formation of DNA–Cr(III)–protein cross-links.^{79,80} However, these reactions were performed in the absence of 1,2-diols, which are crucial for stabilization of Cr(V) in biological media, cells, and animals. The diolato complexes are formed via ligand-exchange reactions of sugars with the Cr(V)-reductant intermediates.^{11,19,28} Furthermore, the formation of reactive Cr(III) species, capable of binding to DNA, also involves Cr(V) intermediates.^{3,49} The isolation and characterization of chromium(V) monosaccharide complexes, reported herein, will allow for the first time more detailed studies of their roles both in the genotoxicity and carcinogenicity of Cr(VI)^{2–5} and in the antidiabetic activity of Cr(III).^{8,9,73}

■ ASSOCIATED CONTENT

■ Supporting Information

UV–vis spectra of Cr(VI/V/IV/III) species in ehbaH₂/ehbaH[–] buffers and their applications to analysis of the Cr(V), Cr(VI), and Cr(III) contents in the reaction mixtures of Cr(VI) with diolato ligands, typical kinetic data for the reactions of Cr(VI) with 1,2-diols and monosaccharides in DMF solutions, application of quantitative EPR spectroscopy for determination of the Cr(V) content in the reaction mixtures, typical ESMS data for fresh aqueous solutions of the isolated reaction products, solid-state EPR spectra (295 K) of the reaction products, application of various models to the simulations of solution EPR spectra of chromium(V) diolato complexes, typical EPR spectra of Cr(V) species generated during the reactions of Cr(VI) with the ligands (Chart 1) in DMF solutions, comparative stability of chromium(V) 1,2-diolato and monosaccharide complexes in unbuffered H₂O, and application of global kinetic analysis for determination of the rate constants of Cr(V) decomposition in aqueous solutions. This material is available free of charge via the Internet at <http://pubs.acs.org>.

■ AUTHOR INFORMATION

Corresponding Author

*E-mail: peter.lay@sydney.edu.au. Tel: 61-2-9351 4269. Fax: 61-2-9351 4269.

Notes

The authors declare no competing financial interest.

■ ACKNOWLEDGMENTS

Financial support of this work was provided by Australian Research Council (ARC) Large and Discovery grants and an Australian Professorial Fellowship to P.A.L. and grants for the ESMS equipment (from ARC) and for the EPR equipment (from ARC and Wellcome Trust). We thank Prof. Nicholas Dixon and Penelope Lilley (Australian National University) for providing pUC9 plasmid DNA.

■ REFERENCES

- (1) Connett, P. H.; Wetterhahn, K. E. *Struct. Bonding (Berlin)* **1983**, *54*, 93–124.
- (2) Sugden, K. D.; Stearns, D. M. *J. Environ. Pathol., Toxicol. Oncol.* **2000**, *19*, 215–230.
- (3) Levina, A.; Codd, R.; Dillon, C. T.; Lay, P. A. *Prog. Inorg. Chem.* **2003**, *51*, 145–250.
- (4) Codd, R.; Irwin, J. A.; Lay, P. A. *Curr. Opinion Chem. Biol.* **2003**, *7*, 213–219.
- (5) Sala, L. F.; Gonzalez, J. C.; Garcia, S. I.; Frascaroli, M. I.; Van, D. S. *Adv. Carbohydr. Chem. Biochem.* **2011**, *66*, 69–120.
- (6) Levina, A.; Lay, P. A. 3.33 Metal Carcinogens. in *Comprehensive Inorganic Chemistry II*; Pecoraro, V., Hambley, T. W., Eds.; Elsevier: New York, 2013; Vol. 33 (Bioinorganic Fundamentals and Applications: Metals in Natural Living Systems and Metals in Toxicology and Medicine); DOI: 10.1016/B978-0-08-097774-4.00333-8.
- (7) Vincent, J. B. *Dalton Trans.* **2010**, *39*, 3787–3794.
- (8) Mulyani, I.; Levina, A.; Lay, P. A. *Angew. Chem., Int. Ed.* **2004**, *43*, 4504–4507.
- (9) (a) Levina, A.; Lay, P. A. *Chem. Res. Toxicol.* **2008**, *21*, 563–571. (b) Lay, P. A.; Levina, A. In *Encyclopedia of Inorganic and Bioinorganic Chemistry*; Scott, R. A., ed.; John Wiley & Sons: Chichester, U.K., 2012; DOI: 10.1002/9781119951438.eibc0040.pub2.
- (10) Zhitkovich, A. *Chem. Res. Toxicol.* **2005**, *18*, 3–11.
- (11) Levina, A.; Harris, H. H.; Lay, P. A. *J. Am. Chem. Soc.* **2007**, *129*, 1065–1075; **2007**, *129*, 9832.
- (12) Rossi, S. C.; Gorman, N.; Wetterhahn, K. E. *Chem. Res. Toxicol.* **1988**, *1*, 101–107.
- (13) Branca, M.; Dessi, A.; Kozlowski, H.; Micera, G.; Serra, M. V. *FEBS Lett.* **1989**, *257*, 52–54.
- (14) Sugiyama, M.; Ando, A.; Ogura, R. *Carcinogenesis* **1989**, *10*, 737–741.
- (15) Appenroth, K. J.; Bischoff, M.; Gabrys, H.; Stoekel, J.; Swartz, H. M.; Walczak, T.; Winnefeld, K. *J. Inorg. Biochem.* **2000**, *78*, 235–242.
- (16) Liu, K. J.; Shi, X.; Jiang, J.; Goda, F.; Dalal, N.; Swartz, H. M. *Ann. Clin. Lab. Sci.* **1996**, *26*, 176–184.
- (17) Sakurai, H.; Takechi, K.; Tsuboi, H.; Yasui, H. *J. Inorg. Biochem.* **1999**, *76*, 71–80.
- (18) Barr-David, G.; Charara, M.; Codd, R.; Farrell, R. P.; Irwin, J. A.; Lay, P. A.; Bramley, R.; Brumby, S.; Ji, J.-Y.; Hanson, G. R. *J. Chem. Soc., Faraday Trans.* **1995**, *91*, 1207–1216.
- (19) Levina, A.; Codd, R.; Lay, P. A. In *High Resolution EPR. Applications to Metalloenzymes and Metals in Medicine (Biological Magnetic Resonance, Vol. 28)*; Hanson, G., Berliner, L., Eds.; Springer: New York, 2009; pp 551–580.
- (20) Farrell, R. P.; Judd, R. J.; Lay, P. A.; Dixon, N. E.; Baker, R. S. U.; Bonin, A. M. *Chem. Res. Toxicol.* **1989**, *2*, 227–229.
- (21) Sugden, K. D.; Wetterhahn, K. E. *Chem. Res. Toxicol.* **1997**, *10*, 1397–1406.
- (22) Levina, A.; Barr-David, R.; Codd, R.; Lay, P. A.; Dixon, N. E.; Hammershøi, A.; Hendry, P. *Chem. Res. Toxicol.* **1999**, *12*, 371–381.
- (23) Codd, R.; Lay, P. A. *J. Am. Chem. Soc.* **1999**, *121*, 7864–7876.
- (24) Codd, R.; Lay, P. A. *J. Am. Chem. Soc.* **2001**, *123*, 11799–11800.
- (25) Codd, R.; Lay, P. A. *Chem. Res. Toxicol.* **2003**, *16*, 881–892.

- (26) Sala, L. F.; Gonzalez, J. C.; Garcia, S. I.; Frascaroli, M. I.; Mangiameli, M. F. *Global J. Inorg. Chem.* **2011**, *2*, 18–38.
- (27) Levina, A.; Lay, P. A. *Coord. Chem. Rev.* **2005**, *249*, 281–298.
- (28) Levina, A.; Zhang, L.; Lay, P. A. *J. Am. Chem. Soc.* **2010**, *132*, 8720–8731.
- (29) (a) Irwin, J. A. Cr(V)–sugar complexes: possible intracellular intermediates of importance to chromate-induced carcinogenesis. Ph.D. Thesis, The University of Sydney, Sydney, Australia, 1998. (b) Irwin, J. A.; Hanson, G. R.; Lay, P. A. manuscripts to be submitted.
- (30) Gonzalez, J. C.; Daier, V.; Garcia, S.; Goodman, B. A.; Atria, A. M.; Sala, L. F.; Signorella, S. *Dalton Trans.* **2004**, 2288–2296.
- (31) Signorella, S.; Garcia, S.; Rizzotto, M.; Levina, A.; Lay, P. A.; Sala, L. F. *Polyhedron* **2005**, *24*, 1079–1085.
- (32) Gonzalez, J. C.; Garcia, S. I.; Bellu, S.; Atria, A. M.; Pelegrin, J. M. S.; Rockenbauer, A.; Korecz, L.; Signorella, S.; Sala, L. F. *Polyhedron* **2009**, *28*, 2719–2729.
- (33) Gonzalez, J. C.; Garcia, S.; Bellu, S.; Peregrin, J. M. S.; Atria, A. M.; Sala, L. F.; Signorella, S. *Dalton Trans.* **2010**, *39*, 2204–2217.
- (34) Mangiameli, M. F.; Gonzalez, J. C.; Garcia, S.; Bellu, S.; Santoro, M.; Caffaratti, E.; Frascaroli, M. I.; Peregrin, J. M. S.; Atria, A. M.; Sala, L. F. *J. Phys. Org. Chem.* **2010**, *23*, 960–971.
- (35) Frascaroli, M. I.; Signorella, S.; Gonzalez, J. C.; Mangiameli, M. F.; Garcia, S.; de Celis, E. R.; Piehl, L.; Sala, L. F.; Atria, A. M. *Polyhedron* **2011**, *30*, 1914–1921.
- (36) Bartholomäus, R.; Harms, K.; Levina, A.; Lay, P. A. *Inorg. Chem.* **2012**, *51*, 11238–11240.
- (37) Shi, L. The in vitro effects of sugars in Cr(VI)-induced cancers. M.Sc. Thesis, The University of Sydney, Sydney, Australia, 2002.
- (38) Shi, L.; Jing, H.; Ren, G.; Levina, A.; Lay, P. *Weisheng Yanjiu* **2006**, *35*, 348–351.
- (39) (a) *A Review of Human Carcinogens. Part C: Arsenic, Metals, Fibres, and Dusts*; IARC Monographs on the Evaluation of Carcinogenic Risks to Humans; International Agency for Research on Cancer: Lyon, France, 2012; Vol. 100. (b) Levina, A.; Lay, P. A. Chromium toxicity—high valent chromium. In *Encyclopedia of Metalloproteins*; Uversky, V. N., Kretsinger, R. H., Permyakov, E. A., Eds.; Springer: New York, 2011; DOI: 10.1007/978-1-4614-1533-6.
- (40) Krumpolc, M.; Roček, J. *J. Am. Chem. Soc.* **1979**, *101*, 3206–3209.
- (41) Judd, R. J.; Hambley, T. W.; Lay, P. A. *J. Chem. Soc., Dalton Trans.* **1989**, 2205–2210.
- (42) Levina, A.; Codd, R.; Foran, G. J.; Hambley, T. W.; Maschmeyer, T.; Masters, A. F.; Lay, P. A. *Inorg. Chem.* **2004**, *43*, 1046–1055.
- (43) *ProKineticist*, version 1.06; Applied Photophysics: Leatherhead, U.K., 1996.
- (44) Bramley, R.; Ji, J.-Y.; Judd, R. J.; Lay, P. A. *Inorg. Chem.* **1990**, *29*, 3089–3094.
- (45) *Win-EPR*, version 2.11; Bruker-Franzen Analytik: Bremen, Germany, 1996.
- (46) Duling, D. R. *J. Magn. Reson. B* **1994**, *104*, 105–110.
- (47) Senko, M. *IsoPro 3.0*; Informer Technologies, Inc.: Sunnyvale, CA, 1998.
- (48) Levina, A.; Lay, P. A.; Dixon, N. E. *Inorg. Chem.* **2000**, *39*, 385–395.
- (49) Levina, A.; Lay, P. A.; Dixon, N. E. *Chem. Res. Toxicol.* **2001**, *14*, 946–950.
- (50) Brauer, S. L.; Hneihen, A. S.; McBride, J. S.; Wetterhahn, K. E. *Inorg. Chem.* **1996**, *35*, 373–381.
- (51) Gez, S.; Luxenhofer, R.; Levina, A.; Codd, R.; Lay, P. A. *Inorg. Chem.* **2005**, *44*, 2934–2943.
- (52) Headlam, H. A.; Lay, P. A. *Inorg. Chem.* **2001**, *40*, 78–86.
- (53) Kaiwar, S. P.; Raghavan, M. S. S.; Rao, C. P. *J. Chem. Soc., Dalton Trans.* **1995**, 1569–1576.
- (54) Signorella, S.; Santoro, M.; Frutos, A.; Escandar, G.; Salas-Peregrin, J. M.; Moreno, V.; González-Sierra, M.; Sala, L. F. *J. Inorg. Biochem.* **1999**, *73*, 93–100.
- (55) Daier, V.; Signorella, S.; Rizzotto, M.; Frascaroli, M. I.; Palopoli, C.; Brondino, C.; Salas-Peregrin, J. M.; Sala, L. F. *Can. J. Chem.* **1999**, *77*, 57–64.
- (56) Signorella, S.; Daier, V.; García, S.; Cargnello, R.; González, J. C.; Rizzotto, M.; Sala, L. F. *Carbohydr. Res.* **1999**, *316*, 14–25.
- (57) Bramley, R.; Ji, J.-Y.; Lay, P. A. *Inorg. Chem.* **1991**, *30*, 1557–1564.
- (58) Codd, R.; Dillon, C. T.; Levina, A.; Lay, P. A. *Coord. Chem. Rev.* **2001**, *216–217*, 533–577.
- (59) Levina, A.; Foran, G. J.; Lay, P. A. *Chem. Commun.* **1999**, 2339–2340.
- (60) Codd, R.; Lay, P. A.; Levina, A. *Inorg. Chem.* **1997**, *36*, 5440–5448.
- (61) Cawich, C. M.; Ibrahim, A.; Link, K. L.; Bumgartner, A.; Patro, M. D.; Mahapatro, S. N.; Lay, P. A.; Levina, A.; Eaton, S. S.; Eaton, G. R. *Inorg. Chem.* **2003**, *42*, 6458–6468.
- (62) Signorella, S.; Daier, V.; Santoro, M.; García, S.; Palopoli, C.; González, J. C.; Korecz, L.; Rockenbauer, A.; Sala, L. F. *Eur. J. Inorg. Chem.* **2001**, 1829–1833.
- (63) Haupt, G. W. *Natl. Bur. Stand. Circ. (U.S.)* **1952**, *48*, 414–423.
- (64) Levina, A.; Zhang, L.; Lay, P. A. *Inorg. Chem.* **2003**, *42*, 767–784.
- (65) Lay, P. A.; Levina, A. *Inorg. Chem.* **1996**, *35*, 7709–7717.
- (66) Da Cruz Fresco, P.; Kortenkamp, A. *Carcinogenesis* **1994**, *15*, 1773–1778.
- (67) Kortenkamp, A.; Casadevall, M.; Faux, S. P.; Jenner, A.; Shayer, R. O. J.; Woodbridge, N.; O'Brien, P. *Arch. Biochem. Biophys.* **1996**, *329*, 199–207.
- (68) Pattison, D. I.; Davies, M. J.; Levina, A.; Dixon, N. E.; Lay, P. A. *Chem. Res. Toxicol.* **2001**, *14*, 500–510.
- (69) Bose, R. N.; Moghaddas, S.; Mazzer, P. A.; Dudones, L. P.; Joudah, L.; Stroup, D. *Nucleic Acid Res.* **1999**, *27*, 2219–2226.
- (70) (a) Zhang, L.; Lay, P. A. *J. Am. Chem. Soc.* **1996**, *118*, 12624–12637. (b) Zhang, L. B.; Lay, P. A. *Aust. J. Chem.* **2000**, *53*, 7–13. (c) Lay, P. A.; Levina, A. *J. Am. Chem. Soc.* **1998**, *120*, 6704–6714.
- (71) Signorella, S.; Lafarga, R.; Daier, V.; Sala, L. F. *Carbohydr. Res.* **2000**, *324*, 127–135.
- (72) Hveding, J. A.; Kjolberg, O.; Reine, A. *Acta Chem. Scand.* **1973**, *27*, 1427–1428.
- (73) Levina, A.; Lay, P. A. *Dalton Trans.* **2011**, *40*, 11675–11686.
- (74) Levina, A.; Bailey, A. M.; Champion, G.; Lay, P. A. *J. Am. Chem. Soc.* **2000**, *122*, 6208–6216.
- (75) Salnikow, K.; Zhitkovich, A. *Chem. Res. Toxicol.* **2008**, *21*, 28–44.
- (76) Brooks, B.; O'Brien, T. J.; Ceryak, S.; Wise, J. P., Sr.; Wise, S. S.; Wise, J. P., Jr.; DeFabo, E.; Patierno, S. R. *Carcinogenesis* **2008**, *29*, 1064–1069.
- (77) Charton, M. *Prog. Phys. Org. Chem.* **1981**, *13*, 119–251.
- (78) Casadevall, M.; Fresco, P. D.; Kortenkamp, A. *Chem.–Biol. Interact.* **1999**, *123*, 117–132.
- (79) Zhitkovich, A.; Song, Y.; Quievryn, G.; Voitkun, V. *Biochemistry* **2001**, *40*, 549–560.
- (80) Macfie, A.; Hagan, E.; Zhitkovich, A. *Chem. Res. Toxicol.* **2010**, *23*, 341–347.